HiSST: 3rd International Conference on
High-Speed Vehicle Science Technology
14 -19 April 2024, Busan, Korea

Transpiration Cooled Fin Flight Experiment FinExII on HIFLIER1

Giuseppe D. Di Martino[1], Jonas Peichl[2],
Fabian Hufgard[3], Christian Dürnhofer[4], Stefan Löhle[5],
Johannes Göser[6]

Abstract

The flight in hypersonic conditions implies important challenges for the vehicle development concerning in first place the thermal protection of the external structures, especially in the presence of sharp edges, where the high heat loads generated by the strong attached shock waves become even more critical. For these applications, a new variant of the C/C-SiC material with defined porosity level has been developed in the past years in order to combine the high-temperature resistance of the CMC material with the transpiration cooling technology. In the present paper, the activities for the flight testing of such technology applied to sharp leading-edge fins in hypersonic conditions is presented. For this purpose, in the framework of the HIFLIER flight research experiment, an experimental module of the sounding rocket was designed and constructed, housing four fins with leading edge made of the new porous CMC material and connected to a nitrogen gas supply system for the transpiration cooling application.

Keywords: *Transpiration Cooling, Ceramic Matrix Composites, Thermal Protection System, Hypersonic Flight*

Nomenclature

AFRL – Air Force Research Laboratory
CATS – Cooling Adjustment for Transpiration Systems
C/C – Carbon/carbon
C/C-SiC – Carbon/Carbon reinforced silicon carbide
CFRP – Carbon fiber reinforced plastic
CMC – Ceramic Matrix Composite
DLR – German Aerospace Center
DLR-BT – DLR Institute of Structures and Design
DLR-MORABA – DLR Mobile Rocket Base
FinExII – Fin Experiment II
FRC – Flow rate control
HEFDiG – High Enthalpy Flow Diagnostics Group
HIFLIER – Hypersonic International Flight Research Experimentation
LSI – Liquid silicon infiltration
NISI3D – 3-Dimensional Non-Integer System Identification
OCTRA – Optimized Ceramic for Transpiration Cooling Application
TC – Thermocouple
TPS – Thermal protection system

[1] *Research scientist, DLR Institute of Structures and Design, Pfaffenwaldring 38-40, 70569 Stuttgart, Germany, Giuseppe.DiMartino@dlr.de*
[2] *Research scientist, DLR Institute of Structures and Design, Pfaffenwaldring 38-40, 70569 Stuttgart, Germany, Jonas.Peichl@dlr.de*
[3] *PhD student, High Enthalpy Flow Diagnostics Group (HEFDiG), Institute of Space Systems, Pfaffenwaldring 29, 70569 Stuttgart, Germany, hufgard@irs.uni-stuttgart.de*
[4] *PhD student, High Enthalpy Flow Diagnostics Group (HEFDiG), Institute of Space Systems, Pfaffenwaldring 29, 70569 Stuttgart, Germany, cduernhofer@irs.uni-stuttgart.de*
[5] *Research scientist, Group leader HEFDiG, Institute of Space Systems, Pfaffenwaldring 29, 70569 Stuttgart, Germany, loehle@irs.uni-stuttgart.de*
[6] *Research scientist, DLR Mobile Rocket Base, Münchener Straße 20, 82234 Weßling, Germany, Johannes.Goeser@dlr.de*

a, c, k – CATS constants
α_n, β_n – NISI3D constants
A_c – transpiration cooling area
K_D – Darcy coefficient
K_F – Forchheimer coefficient
L_{ch} – characteristic length
$\dot{m}$ – mass flow rate
μ – dynamic viscosity
p – pressure
$\dot{q}$ – heat flux
ρ – density
T – temperature
u_D – superficial Darcy velocity

Subscripts
cg – coolant gas
feed – feeding line
in – inlet
out – outlet

1. Introduction

The thermal protection of the external structures represents one of the most challenging requirements for the development of hypersonic flight vehicles, since they are exposed to the harsh thermal loads determined by the forming highly-energetic shock waves.

Typically, these requirements lead to the application of lightweight ceramic matrix composites (CMC), such as C/C-SiC, for thermal protection systems, as they are able to withstand high temperatures. In this framework, the Institute of Structures and Design of the German Aerospace Centre (DLR-BT) has developed a unique expertise for the development of such materials [1], its full characterization as well as the integration and validation as a thermal protection system (TPS) for hypersonic sounding rocket flight experiments, successfully flown for example in SHEFEX I and II [2, 3] and most recently in STORT [4, 5]. Moreover, the usage of this material for stabilizer fin structures could be successfully demonstrated in the FinEx experiment on the HiFire-5 flight experiment [6].

However, in order to overcome the material load limits, in the cases in which the heat fluxes become even more critical, active cooling of the structure could become necessary, e.g. for flight at high Mach numbers or for longer operational time. In this framework, one of the possibilities is represented by the transpiration cooling, which consists in feeding a coolant fluid through a porous wall into the hot gas region, with the double effect of directly cooling the wall itself and mixing into the boundary layer resulting in a lower convective heat flux [7-8].

In order to combine the application of CMC structures with the transpiration cooling technology, the so-called OCTRA (Optimized Ceramic for Transpiration Cooling Application) material was developed at DLR-BT [9], which consists in a variant of the C/C-SiC CMC material with defined porosity level designed specifically for transpiration cooling applications.

In the framework of the flight experiment project Hypersonic International Flight Research Experimentation (HIFLIER), coordinated by the US Air Force Research Laboratory (AFRL) and operated by DLR's Mobile Rocket Base (DLR-MORABA), an experimental module (so called FinExII) of the sounding rocket has been designed and constructed by DLR-BT, in collaboration with the High Enthalpy Flow Diagnostic group (HEFDiG) of the Institute of Space Systems (IRS) at the University of Stuttgart, finalized at the flight test of the abovementioned technologies applied to sharp leading edges in real hypersonic flight conditions.

The present paper will give an overview of the experimental module setup and will preliminarily present some selected measured flight data.

2. FinExII system overview

The general design of the sounding rocket module dedicated to the FinExII experiment is shown in Figure 1, while Figure 2 shows pictures of the FinExII module fully assembled, before its integration on the HIFLIER rocket.

In particular, the module is equipped with four identical fins as shown in Figure 1. For each pair of diametrically opposite fins, which are exposed to the same flow conditions determined by the upstream sounding rocket forebody, one is uncooled as reference and one is cooled in different operating conditions, as it will be described in the following.

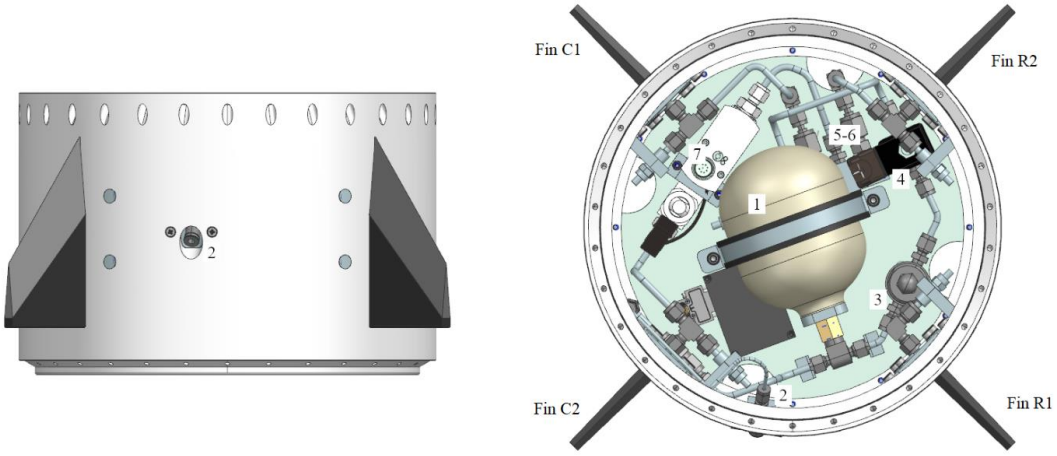

Figure 1: FinExII module overall design.

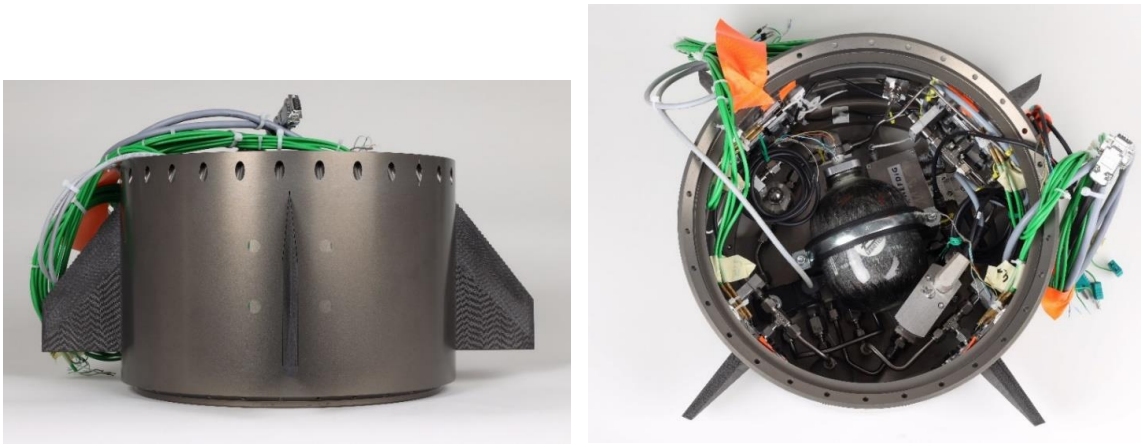

a) Side view **b) Top view**

Figure 2. FinExII module fully assembled.

2.1. CMC fins with porous leading edge for transpiration cooling

Figure 3 shows a schematic of the fin, which is made of two different parts joined together. The leading edge is made of a permeable C/C-SiC material called OCTRA which has a porosity of around 10% [9], while the rest of the fin is made of classical impermeable C/C-SiC. In this way the transpiration cooling is applied only in the region of the leading edge, which is expected to experience the highest thermal loads.

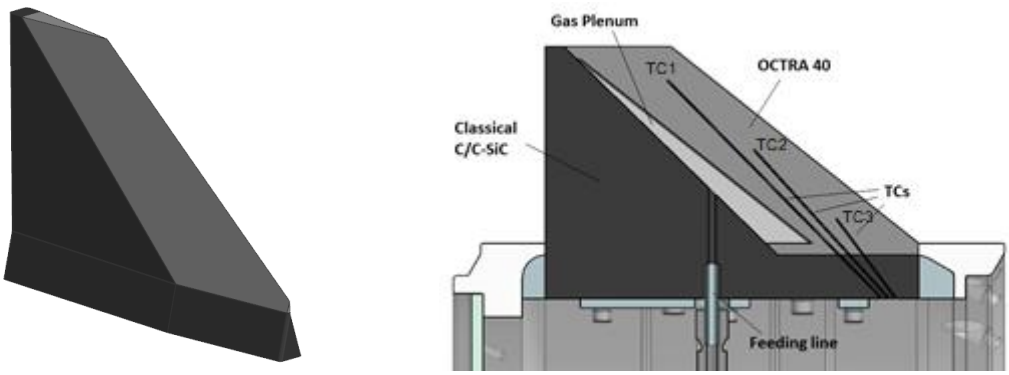

a) Fin isometric view **b) Cut view of the fin integrated in the module**

Figure 3: Fin design.

The CMC fins were manufactured with the Liquid Silicon Infiltration (LSI) method [1]. In particular, for the backward component of the fin a material plate is manufactured via hot pressing and pyrolyzed to the C/C status. In parallel, for the porous leading edge a plate is manufactured also with the hot-pressing method but using fabric plies with carbon and aramid fibres. The latter degrade in the pyrolysis process, generating the C/C plate with a higher porosity which is the basis material for the manufacturing of the OCTRA component. In this work, the so-called OCTRA40 material is used, indicating a 40%vol percentage of aramid fibres in the CFRP preform leading to a porosity of around 10% in the final C/C-SiC state [9]. A detailed description of the fin manufacturing process is given in [10].

A picture of the fin in its final state is shown in Figure 4.

Figure 4: Fin for FinExII.

As the macroscopic porosity pattern of the OCTRA material is defined by the orientation of the fibers in the CFRP preform, the coolant flow direction can be controlled. In fact, using two-dimensional mixed carbon/aramid fiber plies in the manufacturing of the CFRP preform results in a main orientation of the pores parallel to the chosen fiber orientation, which for the case of the fins in the present work is shown in Figure 5.

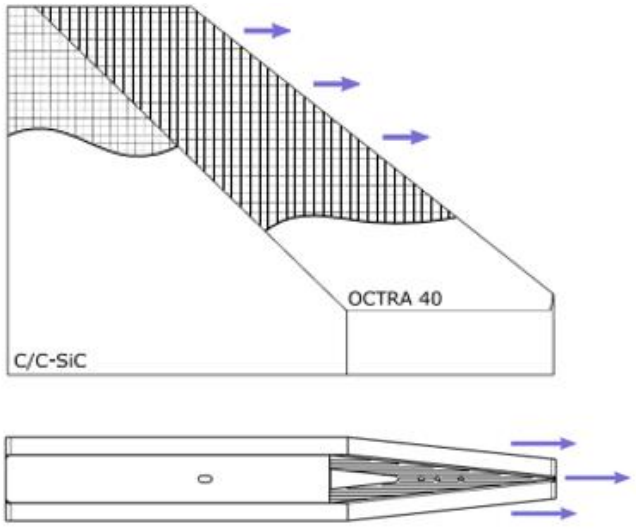

Figure 5: Fin fibres orientation.

The permeability of the fins was preliminary assessed considering the Darcy-Forchheimer equation which is formulated by Innocentini et al. [11] as with the Darcy and Forchheimer coefficients K_D and K_F as the material specific permeation properties.

$$\frac{{p_{cg,in}}^2 - {p_{cg,out}}^2}{2p_{cg,out}L_{ch}} = \left(\frac{\mu_{cg}}{K_D}\right)u_D + \left(\frac{\rho_{cg}}{K_F}\right){u_D}^2 \quad (1)$$

The superficial Darcy velocity u_D can be derived from the coolant mass flow rate via the continuity equation

$$u_D = \frac{\dot{m}_{cg}}{\rho_{cg} A_c} \tag{2}$$

The through-flow behaviour of the transpiration cooled fins was characterized at the AORTA (Advanced Outflow Research Facility for Transpiration Application) facility at DLR-BT [12]. Steady state pressure measurements were conducted using different mass flow rates of nitrogen at ambient temperature to obtain the pressure loss-mass flow curve. K_D and K_F were obtained by fitting the measured data according to Eq. (1), using a "least squares" algorithm. The uncertainties are determined using a Monte-Carlo method with a sample size of 200000.

Assuming $L_{ch} = 38\ \mathrm{mm}$ for the characteristic length and $A_c = 2.69 \cdot 10^{-3}\mathrm{m}^2$ for the area, given by the sum of the projections of the leading edge area in the planes perpendicular to the fibers directions, the resulting Darcy and Forchheimer coefficients determined for both transpiration cooled fins C1 and C2 with their respective uncertainties are given in Table 1. As comparison K_D and K_F for the OCTRA determined from cylindrical samples are also given. The deviation between the values of the coefficients obtained for the fins and the plate can partially be attributed to the complex fin geometry.

Table 1: Darcy and Forchheimer Coefficients of the transpiration cooled fins

	Fin C1	Fin C2	OCTRA cyl. sample [13]
Darcy coefficient K_D, m²	$1.76 \cdot 10^{-12} \pm 1.5 \cdot 10^{-13}$	$1.57 \cdot 10^{-12} \pm 1.2 \cdot 10^{-13}$	$1.62 \cdot 10^{-12}$
Forchheimer coefficient K_F, m	$2.30 \cdot 10^{-8} \pm 1.2 \cdot 10^{-9}$	$2.44 \cdot 10^{-8} \pm 1.4 \cdot 10^{-9}$	$4.5 \cdot 10^{-7}$

2.2. Cooling gas feeding system and nominal operation conditions

Figure 6 shows the schematic representation of the nitrogen gas supply system. The corresponding components in the 3D CAD model, as designed for the FinEx II experiment module, are depicted Figure 1b.

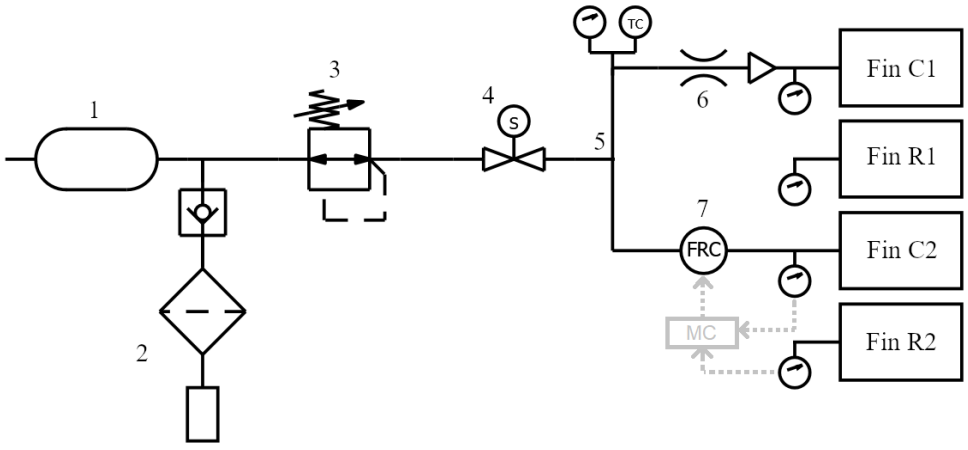

Figure 6: FinExII cooling gas feeding line schematic.

The gas is contained at an initial pressure of 240 bar in a small gas tank (ARMOTECH, 1), which has an internal volume of 800 ml. The filling of the tank is carried out before flight through the filling line (2), including a dedicated intake valve, a Swagelok® filter to avoid any contamination of the gas in the system and a check valve.

A pressure reducer (Swagelok®, 3) set to a specific position before flight reduces the gas pressure to the nominal absolute pressure of 13,7 bar defined for the transpiration cooling. Further downstream, a

solenoid valve (Bürkert 6013, 4) is placed, which is opened via an electric signal during the prescribed experiment windows. The gas flow is then is split in two different lines for fins C1 and C2, respectively, through a dedicated distributor (5). For measuring the gas total pressure and temperature in the feeding system, a combined pressure and temperature sensor (Kulite® HKL-T-312) is mounted to the distributor.

For Fin C1, a constant mass flow rate of the cooling gas is foreseen, which is obtained including along the line a disk with an orifice (6) with a prescribed diameter operating in choked conditions (M=1 at the throat section). The nominal value of the mass flow rate of the coolant gas is defined based on the experience gained in the previous flight experiment AKTiV on SHEFEX II [14].

For the fin C2 a novel approach is considered in which the mass flow rate of the cooling gas is adjusted in real time according to the instantaneous actual thermal load applying the so-called Cooling Adjustment for Transpiration Systems (CATS) method, developed by HEFDiG [15]. For this purpose, a mass flow rate controller (Bronkhorst® IN-FLOW F-201AI, 7) is included, which is in turn controlled by a in which the CATS method is implemented. More details are given in Sec. 2.3.

Combined pressure and temperature sensors (Kulite HKL-T-312 for C1 and Kulite XTL-190SM-700kPaA for C2) are included upstream each fin to measures the corresponding pressure and temperature in the plenum.

Table 2 summarizes the nominal transpiration cooling operating conditions for the different fins.

Table 2: Transpiration cooling operating mass flow rates for the different fins.

Fin R1	Fin C1	Fin R2	Fin C2
No cooling Reference for fin C1	0.85 g/s	No cooling Reference for fin C2	CATS method

The transpiration cooling experiment will be activated on the two cooled fins switching on the coolant mass flow in two different time windows, with a duration of 50 s each, covering the hypersonic flight phase (with Mach numbers up to 6) during the ascent and the descent phases of the rocket flight trajectory, i.e. correspondingly to the peak of the convective heat flux, as it will be shown in Sec. 3.

2.3. Cooling Adjustment for Transpiration Systems applied to FinExII

Cooling Adjustment for Transpiration Systems (CATS) is a method to automatically adjust the cooling of a transpiration cooled wall depending on the real-time measured surface heat flux, derived from exclusively non-intrusive measurements [15], i.e. without any sensor system, which would weaken the structure or perturbate the transpiration cooling itself.

As shown in Figure 6, the CATS system consists of the porous fin, a mass flow rate controller and a pressure gauge to measure the pressure in the plenum. Additionally, the plenum of the uncooled Fin R2 is equipped with a pressure gauge to measure the ambient pressure.

From the measurement of the pressure drop over the transpiration cooled wall, the mean fluid temperature in the transpiration cooled wall can be obtained with the relation of Darcy's law, derived from Eq. (1), neglecting the Forchheimer term, assuming ideal gas behaviour and using a look-up table and the approximation of the viscosity by Sutherland's Law as a function of the temperature.

The calculated temperature and mass flow rate measured by the flow controller are the input variables in the equation to determine the surface heat flux, which is

$$\dot{q}(t) = a\,\frac{dT(t)}{dt} + c\,\dot{m}(t)\,(T(t) - T(0)) \tag{3}$$

The parameters a and c are found using a system identification approach and non-destructive calibration of the actual flight hardware.

The required calculations are computationally cheap and are performed by a microcontroller in real-time. The micro-controller adjusts the setpoint of the mass flow controller depending on the measured heat flux according to

$$\dot{m}_{set}(t) = \dot{m}_{min} + k\,\dot{q}(t) \tag{4}$$

with the minimum mass flow rate $\dot{m}_{min}$ and the proportional factor k. This means that the cooling is boosted at the same time as the heat flux affects the surface. This is particularly useful with regards to the film cooling characteristics of transpiration cooling, which reduces the inbound heat flux proportionally to its magnitude. Thus, the integrated heat load is minimized.

The experimental setup for the CATS calibration is shown in Figure 7. The fin was oriented such that the leading edge pointed towards the optics. Mirrors on each side of the fin reflected the laser light onto both sides of the permeable part simultaneously.

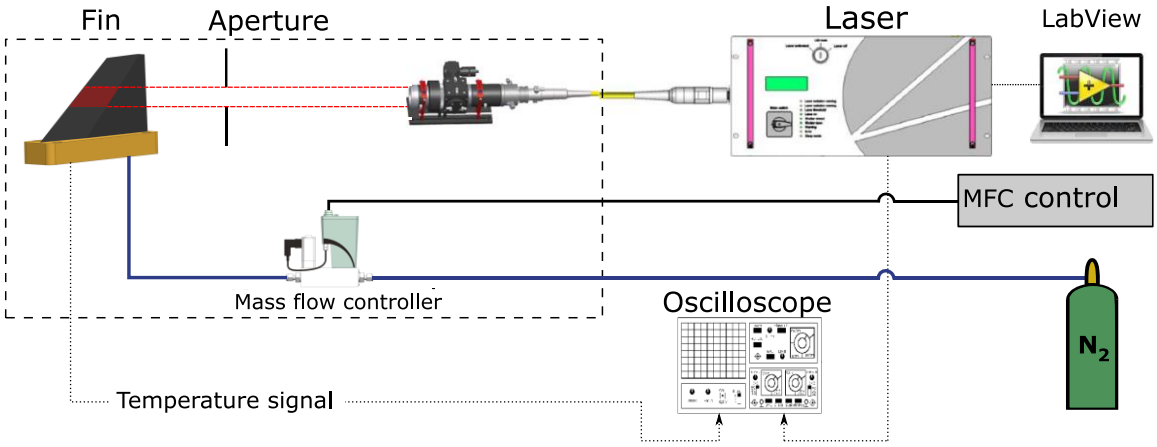

Figure 7: Experimental setup for CATS and NISI calibration (adapted from [16])

The actual flight hardware, including the on-board electronics box for data acquisition, all sensors, the flow controller and the gas tubing downstream of the latter, was used for the CATS calibration (see Figure 8).

Additional information on the CATS calibration process and data can be found in [10].

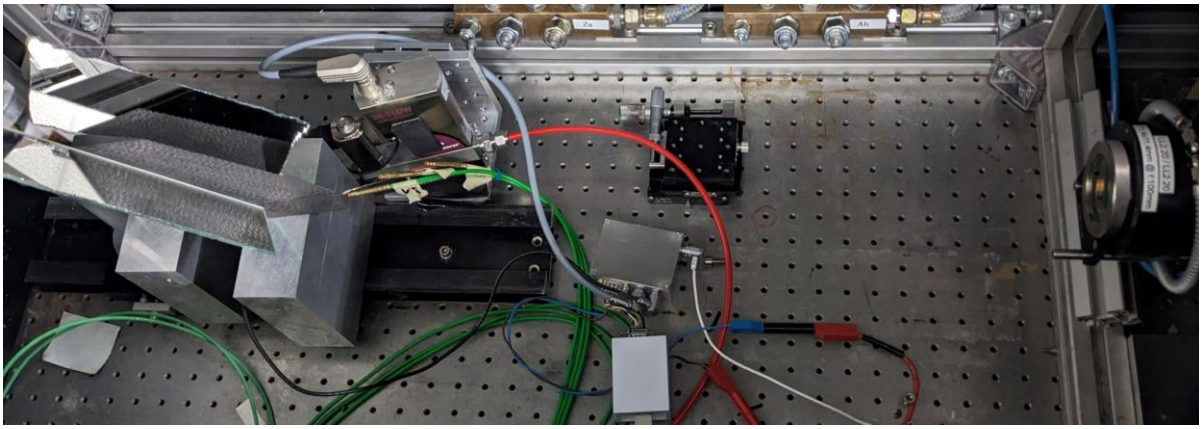

Figure 8: Experimental setup for the CATS calibration.

2.4. Non-Integer System Identification method for spatially resolved heat flux determination

The Non-Integer System Identification (NISI) Method is used for the determination of surface heat flux from an in-depth temperature measurement [17]. The process chain of the NISI method is summarized

in Figure 9. A system identification approach is applied where the heat flux $\dot{q}$ and temperature T are related by

$$\sum_{n=L_0}^{L} \alpha_n \frac{d^{n/2}}{dt^{n/2}} T(t) = \sum_{n=M_0}^{M} \beta_n \frac{d^{n/2}}{dt^{n/2}} \dot{q}(t) \tag{5}$$

The parameters $\alpha_n$and β_n are found from calibration data. In particular, the impulse response is used in the final stage to solve the inverse heat conduction problem, i.e. the determination of the surface heat flux from the measured temperature data, applying common methods as for example the future time algorithm by Beck [18].

This approach can be extended to a set of temperature sensors in order to resolve the determination of surface heat flux into individual areas [19]. We apply this NISI3D approach to the HIFLIER fins, where we will measure the heat flux onto three areas as shown in Figure 10. The number of segments corresponds to the number of temperate measurements. The fins are equipped with three thermocouples each (see Figure 3), so a total of three areas per fin can be calibrated. Since the highest heat flux is expected near the sharp leading edge, the focus is on the resolution of this area. Additionally, thermal conduction between the C/C-SiC and the OCTRA part can be neglected within the measurement time of the system. Therfore, the three areas are discretized solely on the OCTRA leading edge. All areas have the same height of 33 mm and span from the leading edge to the end of the OCTRA part. The temperatures are measured by three thermocouples in each fin.

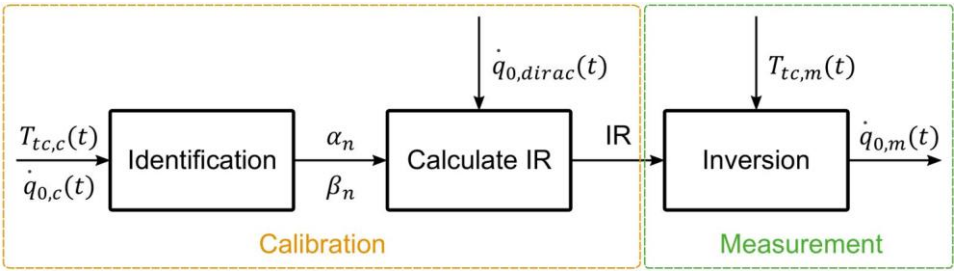

Figure 9: Flow chart of the NISI method.

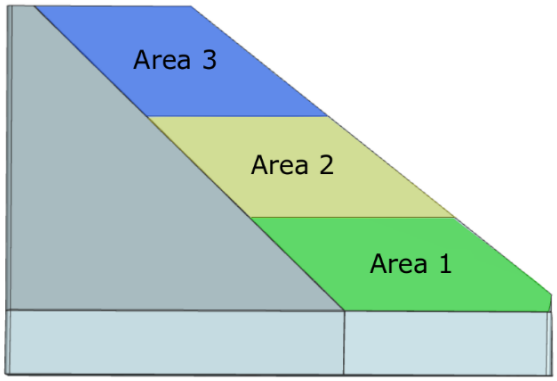

Figure 10: Discretization of fin (adapted from [16])

The experimental setup for the NISI calibration is the same shown in Figure 7. The laser beam is spread homogeneously into a squared spot on the fin. The optical power is calculated from the demand voltage using the manufacturer's specifications. The laser (Laserline LDM 500-100) provides a wavelength of 910 nm. The final heat flux on the fin can then be calculated using the optical power of the laser, the area of the laser spot and the emissivity of OCTRA. The temperatures and optical power are recorded using an oscilloscope (LeCroy WaveSurver 24 Xs-A).

A set of laser pulses is applied to one segment, which causes a temperature response at all thermocouple locations. This is done for all three segments. A system identification procedure is then

used to find all impulse responses. Each fin is a system of nine impulse responses, connecting all segments to each thermocouple.

Additionally, all fins were calibrated with the described methodology with and without cooling. The mass flow controller is the same as presented in subsection 2.2. Fin C2 was calibrated in 0.1 g/s mass flow intervals up to 1 g/s to account for the varying mass flow rate during the mission.

Additional information on the NISI3D calibration process and data can be found in [10].

3. Selected flight data measured on the FinExII module

The FinExII module was integrated on the single-stage, unguided, rail-launched HIFLIER sounding rocket. The HIFLIER rocket was successfully launched from Esrange Space Center in Kiruna (Sweden) on the 10th October 2023. A picture of the HIFLIER rocket during launch is shown in Figure 11.

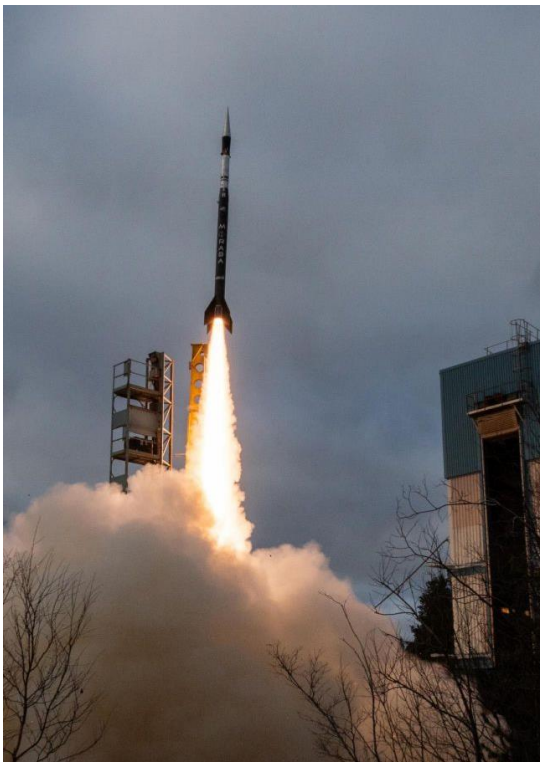

Figure 11: HIFLIER sounding rocket launch (photo credit DLR-MORABA).

The HIFLIER rocket followed a parabolic trajectory with an apogee of 190 km. As mentioned before the transpiration cooling system on the FinExII module was activated in two different time windows of interest, during ascent, between T+5s and T+55s, when the rocket reached a maximum Mach number around 6.2 at an altitude of 22 km, and during descent, between T+365s until motor separation, when the rocket reached a maximum Mach number around 6.1 at an altitude of 25 km.

Since detailed processing and analyses of the flight data are still ongoing, here only some selected preliminary results for fins R1 and C1 will be presented, which nevertheless demonstrate the good operation of the gas system and the effect of the transpiration cooling on the fins thermal behavior.

As mentioned before, the measurement of the pressure and temperature along the gas feeding line allowed to monitor the operation of the transpiration cooling system, as shown in Figure 12, where it can be seen that pressure in the feeding line rises to the value of around 12.5 bar during the prescribed experimental windows. On the other side, the gas temperature shows a slight increase due to the slow heat conduction from the external surfaces to the inner parts of the payload. For the fin C1, a preliminary calibration of the blender allowed the derivation of the mass flow rate of the coolant gas from the measurements of the feeding pressure and temperature, taking into account the pressure loss effect with respect to the case of a de Laval shape. The result is also shown in Figure 12.

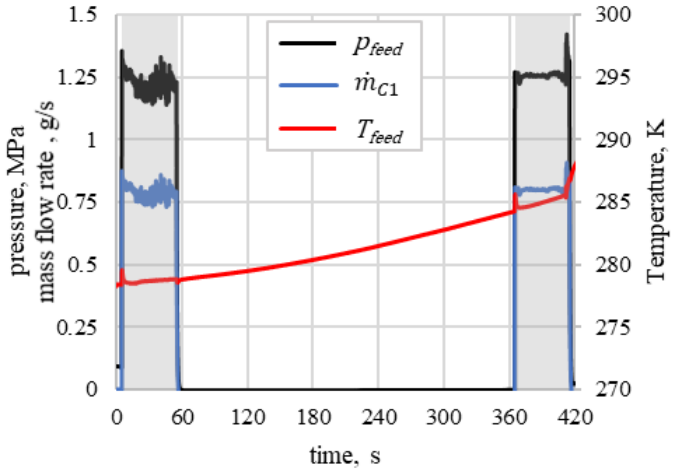

Figure 12. Operating conditions in the FinExII cooling gas system during the flight.

Figure 13 shows the thermal response of the fins R1 and C1 in terms of the measured temperatures in the locations shown in Figure 3b.

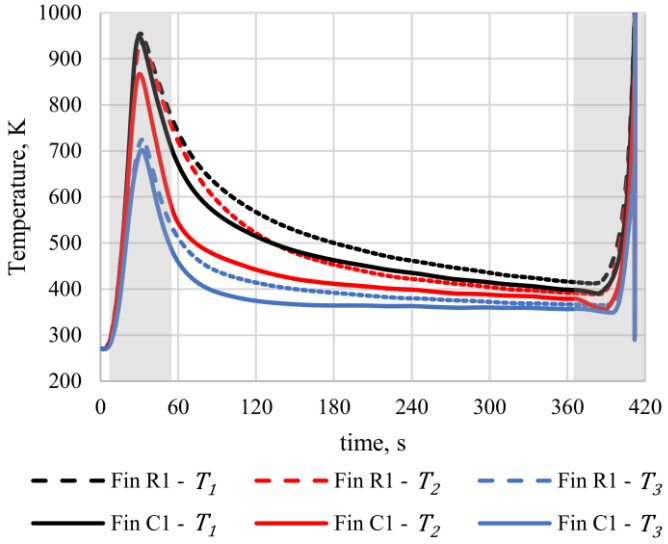

Figure 13. Measured temperature on the Fin R1 and C1.

All the temperatures show a fast increase during the ascent phase reaching the maximum value at around 30 s, to successively decrease when higher altitudes are reached and the Mach number decreases. The temperatures measured on the cooled fin C1 are generally lower, in particular in the central area of the leading edge, corresponding to the TC2 position. On the other side, an interesting behavior is observed for the TC1, where the effect of the cooling is negligible in the first 40 s. This behavior can be possibly associated with the formation of a shock wave on the camera cases present in front of the fins R1 and C1, which impinges on the upper region of the fins creating a localized higher pressure which in turns partially blocks locally the coolant effusion.

4. Numerical reconstruction of the fins' thermal behavior

Collecting experimental flight measurements has a fundamental importance also because they give a precious database for the definition, tuning and validation of numerical models. On the other side the numerical reconstruction of the flight behavior can give important additional information on the fins' thermal response.

Some preliminary results with a simplified approach, focusing on the first experimental window during ascent, are shown in the following.

For the uncooled case, a model similar to the one reported in [10] is used. In particular, the ANSYS Mechanical software was used to solve the transient energy equation with the Finite Element technique on the fin, considering different material properties for the OCTRA leading edge and the backward part made of classical C/C-SiC [13].

The assigned boundary conditions include:

- a convective heat flux on the fin external surface;
- a radiative heat flux from the fin external surface exposed to the ambient, considering for the CMC material an emissivity of 0.85;
- adiabatic condition on the other surfaces.

For the sake of simplicity, in the estimation of the convective heat flux, the fin external surface was split in two parts: the external surface of the leading edge, which has a semi-angle of inclination respect to the upcoming flow of 6° (assuming null angle of attack), and the surface of the backward part which is again parallel to the flow. For each of them constant conditions are assumed. In particular, when supersonic flight is reached, the local flow conditions for the leading edge are assumed to be the conditions downstream the shock waves forming in correspondence of the trajectory conditions at each instant, while a following Prandtl-Meyer expansion is assumed for estimating the flow conditions on the backward part. From the calculated flow conditions, it is then possible to calculate the recovery temperature and, with the correlation formula for laminar flow over a flat plate, the heat transfer coefficient.

The reduction of the heat transfer due to transpiration cooling is modelled using the correlation of Kays et al. [7], which is based on a Couette flow assumption. Refer to [10] for a more detailed description of the model and the governing equations. Here the value $A_c = 2.69 \cdot 10^{-3}\mathrm{m}^2$, defined above, is used, while only around half of the coolant gas mass flow rate, i.e. the coolant flowing in the direction parallel to the flight, is assumed to contribute to the cooling effect.

The results in terms of temperature histories during time at the position of TC2 are shown in Figure 14. It can be observed, that although the considered simplifications, the temperature trends calculated with the numerical simulations show a discrete agreement with the measured values. For the cooled case, the numerical solution underestimates the cooling effect from t=40s on, probably because the contribution of the heat flux removed by advection of the coolant inside the porous material has been here neglected.

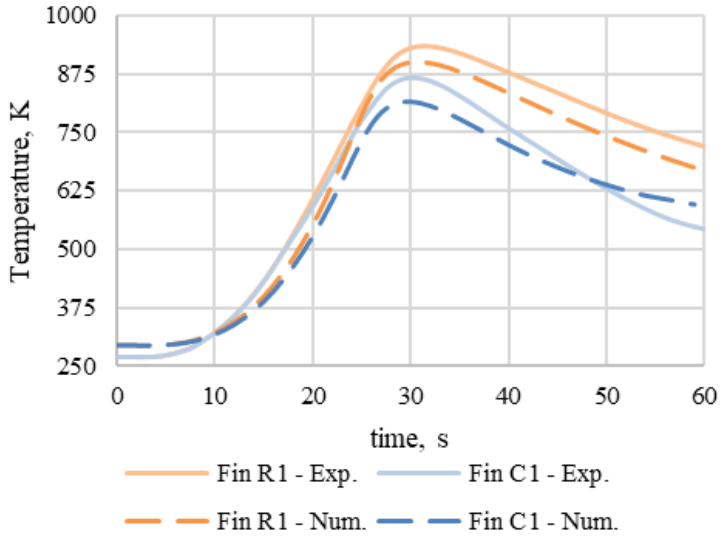

Figure 14: Comparison of numerical results and experimental measures in terms of temperature at the position of TC2.

For the sake of completeness, the temperature distribution calculated through the numerical simulations in the two cases are shown for t=27s, i.e. when maximum temperatures are reached.

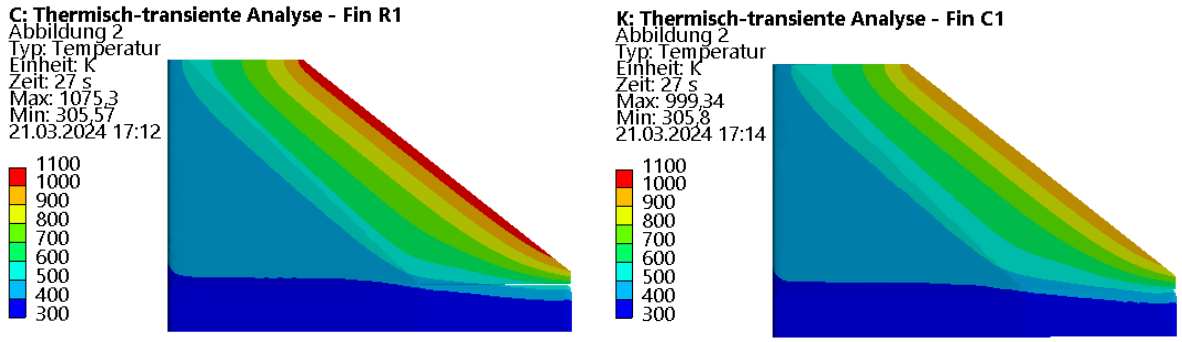

a) Fin R1 **b) Fin C1**

Figure 15: Numerically calculated temperature distributions at t=27s

5. Conclusions

In the framework of the HIFLIER1 flight experiment coordinated by the US AFRL and operated by DLR-MORABA, module of the sounding rocket was designed and setup by DLR-BT in collaboration with HEFDiG. The objective is testing the transpiration cooling technology applied to CMC fins with a sharp leading edge in hypersonic flight regime. For this purpose, the OCTRA material, developed at DLR-BT, consisting in a permeable variant of the C/C-SiC material, is employed at the leading edge of the test fins.

The design of the module, the fins and the coolant gas feeding line are described in this article. In particular, the module is instrumented with four identical fins, of which two will remain uncooled as references, while the other two will be transpiration cooled with different operating conditions. For the Fin C1 a constant mass flow rate of the coolant gas is set, while for the Fin C2 the CATS technique, developed by HEFDiG, for an optimized control of the coolant mass flow rate according to the actual instantaneous thermal load, is implemented and tested. Another part of the experiment foresees the determination of the spatially resolved heat flux acting on the surface by means of the so-called NISI3D method.

The HIFLIER rocket was successfully launched from Esrange Space Center in Kiruna (Sweden) on the 10th October 2023 and the FinExII system operated correctly allowing to receive precious data for a better understanding of the in-flight behavior. Some preliminary selected data have been shown together with preliminary simplified numerical reconstructions, allowing a first insight on the fins' thermal response. The results highlight that the technology worked and showed good potential, while further activities are already going on. These includes the reconstruction of the actual spatially-resolved heat fluxes from the measured temperatures with the Non-Integer System Identification method, the detailed analysis of the CATS system operation for the adjustment of the cooling gas mass flow rate according to the actual thermal load is analyzed in detail and the refinement of the numerical model for simulating the transpiration cooling in-flight behavior.

References

1. Hald, H., Weihs, H.: Safety Aspects of CMC Materials and Hot Structures. Proceedings of Joint ESA-NASA Space-Flight Safety Conference, ESA SP-486 (2002).
2. Weihs, H., Longo, J., Gülhan, A.: Sharp Edge Flight Experiment SHEFEX. Fourth European Workshop on Thermal Protection Systems and Hot Structures Conference Proceedings, ESA SP-521 (2002).
3. Weihs, H., Longo, J., Turner, J.: The Sharp Edge Flight Experiment SHEFEX II, a Mission Overview and Status. 15th AIAA International Space Planes and Hypersonic Systems and Technologies Conference, AIAA 2008-2542 (2008). https://doi.org/10.2514/6.2008-2542
4. Gülhan, A., Hargarten, D., Zurkaulen, M., Klingenberg, F., Siebe, F., Willems, S., Di Martino, G., Reimer, T.: Selected results of the hypersonic flight experiment STORT. Acta Astronaut., 211, 333-343 (2023). https://doi.org/10.1016/j.actaastro.2023.06.034

5. Reimer, T., Di Martino, G., Petkov, I., Dauth, L., Baier, L., Gülhan, A., Klingenberg, F., Hargarten, D.: Design, Manufacturing and Assembly of the STORT Hypersonic Flight Experiment Thermal Protection System. 25th AIAA International Space Planes and Hypersonic Systems and Technologies Conference, AIAA 2023-3089 (2023). https://doi.org/10.2514/6.2023-3089
6. Böhrk, H., Löhle, S., Fuchs, U., Elsäßer, H., Weihs, H.: FinEx – Fin Experiment on HIFiRE-5. 7th Symposium on Aerothermodynamics for Space Vehicles (2011).
7. Kays, W. M.: Heat transfer to the transpired turbulent boundary layer. Int. J. Heat and Mass Transf., 15 (5), 1023–1044 (1972). https://doi.org/10.1016/0017-9310(72)90237-2
8. Glass, D. E., Dilley, A. D., Kelly, H. N.: Numerical analysis of convection/transpiration cooling. J. Spacecrafts and Rockets, 38 (1), 15–20 (2001). https://doi.org/10.2514/2.3666
9. Dittert, C., Kütemeyer, M.: Octra - Optimized Ceramic for Hypersonic Application with Transpiration Cooling. Ceram. Transactions, 263, 389-399 (2017). https://doi.org/10.1002/9781119407270.ch37
10. Di Martino, G., Peichl, J., Hufgard, F., Duernhofer, C., Loehle, S.: Setup of flight experiment of transpiration cooled sharp edge fins on the sounding rocket HIFLIER1. Aerospace Europe Conference 2023 – 10TH EUCASS – 9TH CEAS (2023). doi: 10.13009/EUCASS2023-005
11. Innocentini, M.D.M., Nascimento L.A., Pandolfelli, V.C.: The pressure-decay technique for air permeability evalulation of dense refactory ceramics. Cerment and Concrete Research 34, 293-298 (2004). https://doi.org/10.1016/j.cemconres.2003.08.006
12. Peichl, J., Schwab. A., Selzer, M., Böhrk, H., van Wolfersdorf, J.: Innovative Cooling for Rocket Combustion Chambers. Future Space-Transport-System Components under High Thermal and Mechanical Loads Notes on Numerical Fluid Mechanics and Multidisciplinary Design (146). Springer Nature. Cham, Switzerland (2021).
13. Di Martino, G.D., Böhrk, H., Joelle, S., Müller, C., Peichl, J., Hufgard, F., Duernhofer, C., Loehle, S.: Design of the Transpiration Cooled Fin Experiment FinEx II on HIFLIER1. 2nd International Conference on High-Speed Vehicle Science Technology (2022).
14. Böhrk, H.: Transpiration cooling at hypersonic flight – AKTiV on SHEFEX II. 11th AIAA/ASME Joint Thermophysics and Heat Transfer Conference, AIAA 2014-2676 (2014).
15. Hufgard, F., Duernhofer, C., Loehle, S., Schweikert, S., Müller, C., Di Martino, G., Böhrk, H., Steelant, J., Fasoulas, S.: Adjusting Transpiration Cooling to Real Time Surface Heat Flux Estimation. 2nd International Conference on High-Speed Vehicle Science Technology (2022).
16. Müller, C.: Investigation of the thermal behavior of a transpiration-cooled ceramic fin for HIFLIER1 with inverse heat conduction methods. Master's thesis, Institute of Space Systems, University of Stuttgart, IRS-22-S-035 (2022).
17. Loehle, S.: Derivation of the non-integer system identification method for the adiabatic boundary condition using Laplace transform. Int. J. of Heat and Mass Transf., 115, 1144-1149 (2017). https://doi.org/10.1016/j.ijheatmasstransfer.2017.08.007
18. Beck, J.V., Blackwell, B., St. Clair Jr., C.R.: Inverse Heat Conduction: Ill-posed Problems. John Wiley & Sons, Inc., New York (1985).
19. Dürnhofer, C., Hufgard, F., Fasoulas, S., Loehle, S.: Investigation of Spatially Resolved Heat Flux Determination from In-Depth Temperature Data. 2nd International Conference on Flight Vehicles, Aerothermodynamics and Re-entry Missions & Engineering (FAR) (2022).